BMC Cancer

RESEARCH

Open Access

HLA class II-restricted T cell epitopes in public neoantigens of *ESR1* and *PIK3CA* in breast cancer

Yukari Ando[1,2], Hiroko Miyadera[2*], Hiroko Bando[3], Sachie Hashimoto[3], Emiko Noguchi[2] and Hisato Hara[3]

Abstract

Background The high occurrence of treatment resistance in patients with hormone receptor-positive (HR+) breast cancer is a global health concern. Thus, effective immunotherapy must be developed. The public neoantigens, estrogen receptor 1 (*ESR1*) and phosphatidylinositol-4,5-bisphosphate 3-kinase catalytic subunit alpha (*PIK3CA*), shared by HR+ and endocrine-resistant breast cancer, could be ideal targets for immunotherapy; however, their presentation by human leukocyte antigen class II (HLA II) and recognition by CD4+T cells remain largely unknown.

Methods Seven mutations in *ESR1* and ten mutations in *PIK3CA* were subjected to major histocompatibility complex (MHC)-peptide binding analysis and enzyme-linked immunospot (ELISPOT) assays using peripheral blood mononuclear cells (PBMCs) from healthy donors carrying DRB4*01:03, or DRB4*01:03 and DPA1*02:02-DPB1*05:01 (DP5). DRB4*01:03- or DP5-restricted peptides were inferred from binding measurements and ELISPOT assays. Other DRB1 alleles that can also present these mutant peptides were identified using binding measurements.

Results Positive IFN-γ responses by CD4+T cells were detected for most peptides. The peptides that contain ESR1 (E380Q) and PIK3CA (N345K, E542K, E545K/A, E726K, H1047R/L/Y, and G1049R) are presumably restricted by DRB4*01:03, which is frequently found globally (carrier frequency: 35–63%), or by DRB4*01:03 and DRB1*04 alleles. Some PIK3CA (H1047R/L/Y) peptides can also be presented by DRB1*01:01, DRB1*09:01, DRB1*11:01, and DRB1*15:02. ESR1 (Y537S/N, D538G) peptides are potentially restricted by DP5, a frequently found allele in East Asian populations, and DRB1*01:01 and DRB1*15:01.

Conclusions Mutations in *ESR1* and *PIK3CA* were recognized by CD4+T cells from healthy donors through potential restriction by common HLA II alleles. Further studies are warranted to elucidate the landscape of HLA II presentation and validate the clinical applicability of these mutations for the immunotherapy of patients with endocrine-resistant breast cancer.

Keywords Breast neoplasms, Cancer vaccines, Epitopes, T-Lymphocyte, Histocompatibility antigen class II, Neoantigen

*Correspondence:
Hiroko Miyadera
miyaderah@md.tsukuba.ac.jp
[1] Department of Breast and Endocrine Surgery, Graduate School of Comprehensive Human Sciences, University of Tsukuba, Ibaraki, Japan
[2] Department of Medical Genetics, Institute of Medicine, University of Tsukuba, 1-1-1 Tennodai, Tsukuba, Ibaraki 305-8575, Japan
[3] Department of Breast and Endocrine Surgery, Institute of Medicine, University of Tsukuba, Ibaraki, Japan

Background

Breast cancer is the leading cause of cancer-related deaths worldwide [1]. Hormone receptor-positive (HR+) breast cancer accounts for approximately 70% of all cases of breast cancer [2]. Despite advances in endocrine therapies, treatment resistance remains a challenge, resulting in limited treatment options and poor prognosis in a substantial number of patients [3]. HR+breast neoplasm has been considered a "cold" tumor with low tumor mutational burden (TMB) [4], and thus, is a challenging target for immunotherapy [5]. However, TMB does not always correlate with response to immune checkpoint inhibitors (ICIs) [6], and mRNA-based neoantigen vaccines can enhance immunotherapy in combination with ICIs in cancers with low TMB cancers [7–9], indicating that public neoantigens in HR+breast cancer might be targeted by immunotherapy.

Mutations in estrogen receptor 1 (*ESR1*) and phosphatidylinositol-4,5-bisphosphate 3-kinase catalytic subunit alpha (*PIK3CA*) are major drivers of treatment resistance in HR+breast cancer [10]. *ESR1* mutations are observed in 30–40% of patients resistant to endocrine therapies such as aromatase inhibitors [11]. *ESR1* encodes estrogen receptor alpha (ERα), a member of the nuclear hormone receptor family, and regulates the genes involved in cell proliferation and differentiation [3]. ERα is crucial for hormone-sensitive tumor growth of breast and endometrial cancers [12, 13]. Mutation hotspots in *ESR1* are found within the ligand-binding domain and contribute to hormone-independent tumor growth [14]. *PIK3CA* mutations are found in approximately 30% of breast cancers and in endometrial and colorectal cancers [15, 16]. *PIK3CA* encodes for the p110α subunit of class I phosphatidylinositol 3-kinase (PI3K), an important factor of the PI3K/AKT/mammalian target of rapamycin (mTOR) pathway [17]. Mutations in *PIK3CA* accumulate within the kinase and helical domains [18].

ESR1 and *PIK3CA* mutations are often shared by patients with HR+breast cancer with poor prognosis and are considered public neoantigens because they contribute to the formation of a "hot" immune environment [19–21] through recognition by T cells. In fact, CD8+T cell responses for ESR1 (E380Q, Y537S, D538G) in human leukocyte antigen (HLA)-A2-positive donors [22], ESR1 (Y537S/N) in breast cancer patients [23], ESR1 (Y537S/N/C, D538G) in healthy donors and breast cancer patients [24], and PIK3CA (H1047L) in HLA-A*03:01 or A*11:01-positive healthy donors [25, 26] have been reported; however, CD4+T cell responses and HLA class II (HLA II) restriction patterns of these mutations remain largely unknown. T helper (Th) cells play pivotal roles in cancer immunosurveillance [27] and the induction of strong antitumor immune responses against neoantigens [28–34]. Vaccines targeting both HLA I and II in combination with ICIs are considered one of the most promising immunotherapeutic approaches [35]. HLA II-restricted neoantigen epitopes have been identified in head and neck squamous cell carcinoma and melanoma [36, 37] but not fully explored in breast cancer.

To identify the hotspot mutations of *ESR1* and *PIK3CA* that can be presented by common HLA II and recognized by CD4+T cells, we analyzed HLA II binding and CD4+T cell responses of *ESR1* and *PIK3CA* mutations through MHC-peptide binding measurements and enzyme-linked immunospot (ELISPOT) assays, respectively. The peripheral blood mononuclear cells (PBMCs) from healthy donors were used for the ELISPOT assays. HLA restriction was inferred based on penetrance, binding measurements, and the presence of binding motifs.

Methods

ESR1 and *PIK3CA* mutations

Hotspot mutations in *ESR1* and *PIK3CA* were selected from the Catalog of Somatic Mutations in Cancer (COSMIC) database (https://cancer.sanger.ac.uk/cosmic), a comprehensive resource for exploring somatic mutations in cancer [38], based on COSMIC_Count, which indicated the number of reports of specific mutations in the COSMIC database.

HLA II alleles

DRB4*01:03 and DPA1*02:02-DPB1*05:01 (DP5) were used for the MHC-density assay. These alleles are frequently found in East Asians: DRB4*01:03 (allele frequency: 32.7%, carrier frequency: 54.7%) [39] and DPB1*05:01 (allele frequency: 34.2–37.4%, carrier frequency: 56.7–60.8%) [40]. The following *DRB1* alleles were also used in the MHC-density assay: DRB1*01:01, DRB1*03:01, DRB1*04:01, DRB1*04:05, DRB1*07:01, DRB1*09:01, DRB1*11:01, DRB1*12:01, DRB1*13:01, DRB1*15:01, and DRB1*15:02. These alleles have been frequently detected in several populations. The carrier frequencies of these alleles were calculated from the following datasets in the allelefrequencies.net database [41]: European (USA NMDP European Caucasian (n=1,242,890)), Hispanic (USA Hispanic pop 2 (n=1,999)), East Asian (China Hubei Han (n=3,732)), Southeast Asian (Malaysia Peninsular Malay (n=951)), South Asian (India Central UCBB (n=4,204)), Middle Eastern (Saudi Arabia pop 6 (n=28,927)), and African American (USA NMDP African American pop 2 (n=416,581)). The frequency of DRB4*01:03 indicates the combined frequency of DRB4*01:01 and DRB4*01:03, calculated as the sum of the linked DRB1 alleles.

Binding prediction

The binding of HLA II and peptides was predicted using NetMHCIIpan-4.1 (https://services.healthtech.dtu.dk/services/NetMHCIIpan-4.1/) [42] for HLA II and NetMHCpan-4.1 (https://services.healthtech.dtu.dk/services/NetMHCpan-4.1/) [43] for HLA class I (HLA I). NetMHCIIpan was trained on the binding affinity dataset and eluted ligand mass spectrometry data [42, 43]. The binding of the peptides was predicted as %Rank, with lower %Rank values indicating stronger binding. %Rank < 2 and < 10 were used as the threshold values for strong and weak binders, respectively. The 15-mer peptide region was designed to contain the preferred binding motifs for DRB4*01:03 or A*24:02 according to NetMHCIIpan.

Measurement of HLA-peptide binding by MHC-density assay

The binding of the peptide to HLA II was measured by the MHC-density assay, as described previously [44]. Briefly, HLA-DRα subunit stable cells (DRA) were established through the retrovirus-mediated NIH3T3 cell transduction using pMXs-puro [45] and the packaging cell line PLAT-E [46]. The DRB1- or DRB4-peptide fusion constructs was inserted into pMXs-IG, which carried *IRES* and *GFP* downstream of *DRB1* [47], and were transiently expressed in DRA-stable cells. HLA-DPα subunit stable cells were also established and transduced with a retrovirus that contained DPB1*05:01-peptide fusion constructs. Forty-eight hours after the transduction of the β subunit, cells were collected and stained with anti-pan-HLA II β mAb (clone WR18; Cat# MCA477, Bio-Rad Laboratories, Inc) in the dark at 4°C for 20 min. The cells were washed in 500 µL of flow cytometry (FCM) buffer (PBS, 0.1% BSA), stained with Goat F(ab')2 anti-mouse Ig, human ads-PE (Cat# 1012–09, Southern Biotechnology Associates Inc), and subjected to FCM analysis. The median fluorescence intensity (MFI) of cell surface HLA II expression and cytosolic GFP was measured using SA3800 (Sony Imaging Products & Solutions Inc.). The ratio of MHC to GFP expression, as measured by the MFI, was determined. The MHC-to-GFP expression ratio for the test peptide was normalized to the ratio measured for the negative control peptide g15 (15-mer of glycine) (g15 ratio) and used as an indicator of cell surface expression of the MHC-peptide complex (Miyadera et al. manuscript in preparation). FCS Express 6 software (6.06.0022; De Novo Software) was used for data analysis. The MHC-density assay for each peptide was conducted in > 3 wells. Double-stranded DNA oligonucleotides encoding the signal sequences and peptides were synthesized by Eurofins Genomics (Tokyo, Japan). The NIH3T3 cell line was obtained from RIKEN Bioresource Center.

PBMCs from healthy individuals

The HLA of healthy donors (donor 1 to donor 8) was determined using the PCR-SSO method (GenoDive Pharma, Kanagawa, Japan). PBMCs were isolated from the whole blood using Vacutainer CPT™ (Becton Dickinson, Tokyo, Japan) and preserved in liquid nitrogen with CELLBANKER® 1 (ZENOGEN PHARMA, Fukushima, Japan). Written informed consent was obtained from all participating healthy donors. This study was approved by the Clinical Research Ethics Review Committee of the Tsukuba University Hospital (H29-069).

Generation of mDCs and T cell co-culture

CD14 + cells were magnetically separated from PBMCs using CD14 beads (Miltenyi Biotec, Bergisch Gladbach, Germany) and differentiated into mature dendritic cells (mDCs) using a human monocyte-derived dendritic cell differentiation kit (R&D Systems, Minneapolis, MN, USA) following the manufacturer's instructions. CD14 + cells (1×10^6 cells/mL) were resuspended in serum-free differentiation medium and cultured in a 24-well tissue culture plate with recombinant human interleukin-4 (IL-4) and recombinant human granulocyte–macrophage colony-stimulating factor (GM-CSF) at 37°C in a humidified incubator with 5% CO_2. Half of the medium was replaced every 2–3 days. Recombinant human tumor necrosis factor-alpha (TNF-α) was added on day 7. mDCs were harvested and used as antigen-presenting cells on day 9. T cells were cultured in AIM-V medium (Gibco, Thermo Fisher Scientific, Waltham, MA, USA) supplemented with 5% human male AB serum (Sigma-Aldrich, St. Louis, MO, USA) in a 24-well tissue culture plate. CD8 + T cell-depleted PBMCs were prepared from the PBMCs using CD8-microbeads (Miltenyi Biotec, Bergisch Gladbach, Germany) ($1 - 5 \times 10^5$ cells/mL) and co-cultured with mDCs ($0.1 - 2 \times 10^4$ cells/mL) pretreated with mitomycin C (10 µg/mL) (Nacalai Tesque, Kyoto, Japan) for 1 h. The synthetic mutant and wild-type (wt) peptides (GenScript, Piscataway, NJ, USA) were dissolved in DMSO and added to the co-culture at the final concentration of 10 µM. PBMCs were restimulated with mDCs and peptides on day 8. Recombinant human interleukin-2 (IL-2) (10U/ml) (BioLegend, San Diego, CA, USA) was added after day 3. The medium was replaced every 2–3 days. PBMCs were harvested and subjected to ELISPOT assay after one to three rounds of restimulation.

ELISPOT assay

The ELISPOT assay was conducted using the human interferon-gamma (IFN-γ)/IL-2 double-color ELISPOT kit (Cellular Technology Limited, Cleveland, OH,

USA), following the manufacturer's instructions. The CPI antigen pool (2.5 μg/mL; Cellular Technology Limited, Cleveland, OH, USA) and DMSO were utilized as positive and negative controls, respectively. The 96-well strip ELISPOT plates were precoated with human IFN-γ and IL-2 capture antibodies overnight and blocked with medium for at least 1 h before seeding the cells. T cells were washed with RPMI-1640 (FUJIFILM Wako Pure Chemical Corporation, Osaka, Japan) and co-cultured with mDCs ($0.1 - 2 \times 10^4$ cells/mL) and the peptides for 48 h. IFN-γ and IL-2 production was detected following the manufacturer's protocol. An ImmunoSpot S6 analyzer (Cellular Technology Limited, Cleveland, OH, USA) was used to scan the ELISPOT plates. The threshold for the positive response was set at > 6 spots of IFN-γ per 100,000 PBMCs and at least a two-fold increase in spot number over the background [48, 49]. The assay was performed up to seven times for donor 1 and once or twice for donors 2–8, depending on the availability of PBMCs.

Flow cytometry analysis

Antigen-specific CD4 + T cells collected from ELISPOT plates were expanded in the presence of Dynabeads human T-activator CD3/CD28 (Thermo Fisher Scientific, Waltham, MA, USA). T cells were cultured in AIM-V medium supplemented with recombinant human IL-2 (BioLegend, San Diego, CA, USA) for 2–3 weeks, following the manufacturer's protocol. For FCM analysis, the cells were incubated with Clear Block (Human Fc receptor blocking reagent; MBL, Aichi, Japan) and stained with PE anti-human CD4 antibody (clone OKT4) (BioLegend, San Diego, CA, USA) and FITC anti-human CD8a antibody (clone RPA-T8) (BioLegend, San Diego, CA, USA) in the dark at 4 °C for 30 min. The cells were washed in 500 μL of FCM buffer (PBS, 0.1% BSA) and stained with 7-AAD (BioLegend, San Diego, CA, USA) before FCM analysis.

Statistical analysis

The difference in the g15 ratio between the wt and mutant peptides in the MHC-density assay was assessed using the *t*-test. Statistical significance was set at $p < 0.05$.

Results

Measurement of HLA II peptide presentation

Seven peptides for ESR1 (Fig. 1A, Table S1) and 10 peptides for PIK3CA (Fig. 1B, Table S2), each containing highly frequent mutations according to the COSMIC database, were designed to form a 15-mer peptide based on the %Rank predicted by NetMHCIIpan-4.1 (for DRB4*01:03) and NetMHCpan-4.1 (A*24:02) (Table 1) and used for the MHC-density and ELISPOT assays. The MHC-density assay was used to measure the cell-surface expression of the MHC II β subunit-peptide fusion complex, which is expressed on the surface of MHC II α subunit-stable cell line. The amount of cell-surface MHC II-peptide complex (for the test peptide) was determined by flow cytometry, and its ratio to the amount of MHC II-peptide complex (for the negative control peptide, g15) was calculated. This ratio (the g15 ratio) was used as an indicator of MHC II-mediated antigen presentation (Miyadera, et al. manuscript in preparation). A peptide with a g15 ratio > 2.0 was considered a strong binder.

The MHC-density assay for DRB4*01:03 revealed the binding of two ESR1-peptides and eight PIK3CA-peptides with a g15 ratio > 2.0. Strong binding to DP5 was observed for five ESR1-peptides and none of PIK3CA-peptides (Fig. 2A). Among the mutant peptides with a g15 ratio > 2.0, a significantly higher g15 ratio than that of the wt peptides was observed for ES#1_K303R, ES#2_E380Q, PIK#3_E542K, PIK#4_E545K, PIK#5_E545A (DRB4*01:03), and ES#3_S463P (DP5) (Fig. 2B–E, marked with asterisks).

ELISPOT assay and estimation of HLA II restriction

Next, we performed an ELISPOT assay to identify the peptides that can be recognized by CD4 + T cells, using PBMCs from HLA-typed healthy donors (eight donors carrying DRB4*01:03, among whom four donors also carried DP5) (Table S3). The CD8 + cells-depleted fraction was co-cultured with autologous mDCs, restimulated with mDCs and peptides, and subjected to an ELISPOT assay. The assay was performed up to seven times for donor 1 and once or twice for donors 2–8. Representative ELISPOT data for ES#2_E380Q, PIK#5_E545A, PIK#8_H1047L, and PIK#9_H1047Y are displayed in Fig. 3A. The reproducibility of the positive response, assessed for donor 1, was 1/7 to 6/6 (0.14–1.0, average 0.53), with substantial inter-experimental variation in the spot count, presumably reflecting day-to-day variation in the immune condition (Fig. 3A, Table S4). The penetrance of ELISPOT positive peptides (for donors 1–8) was 1/4 to 3/4 (0.25 to 0.75, average 0.50) (Table S5). The peptide pairs (wt and mutant peptides) that contained peptide(s) with a penetrance ≥ 0.4 in the ELISPOT assay and g15 ratio > 2.0 for DRB4*01:03 and DP5 are presented in Fig. 3B and C, respectively. Most peptides with a g15 ratio > 2.0 (Fig. 3B) contained an anchor motif for DRB4*01:03 (P1 (Ile, Leu, and Val), P4 (Gln and Glu), P6 (Leu, Val, and Ile), and P7 (Asp and Glu)) [42], except for ES#1_K303R. The DRB4*01:03 anchor motif was also found in PIK#6_E726K, which showed penetrance ≥ 0.4 and g15 ratio = 1.5 (Fig. 4A). Based on these findings, the peptides shown in Fig. 4A (ES#2_E380Q, PIK#1_N345K, PIK#3_E542K, PIK#4,5_E545K/A, PIK#6_E726K, PIK#7–9_H1047R/L/Y, and PIK#10_G1049R) were

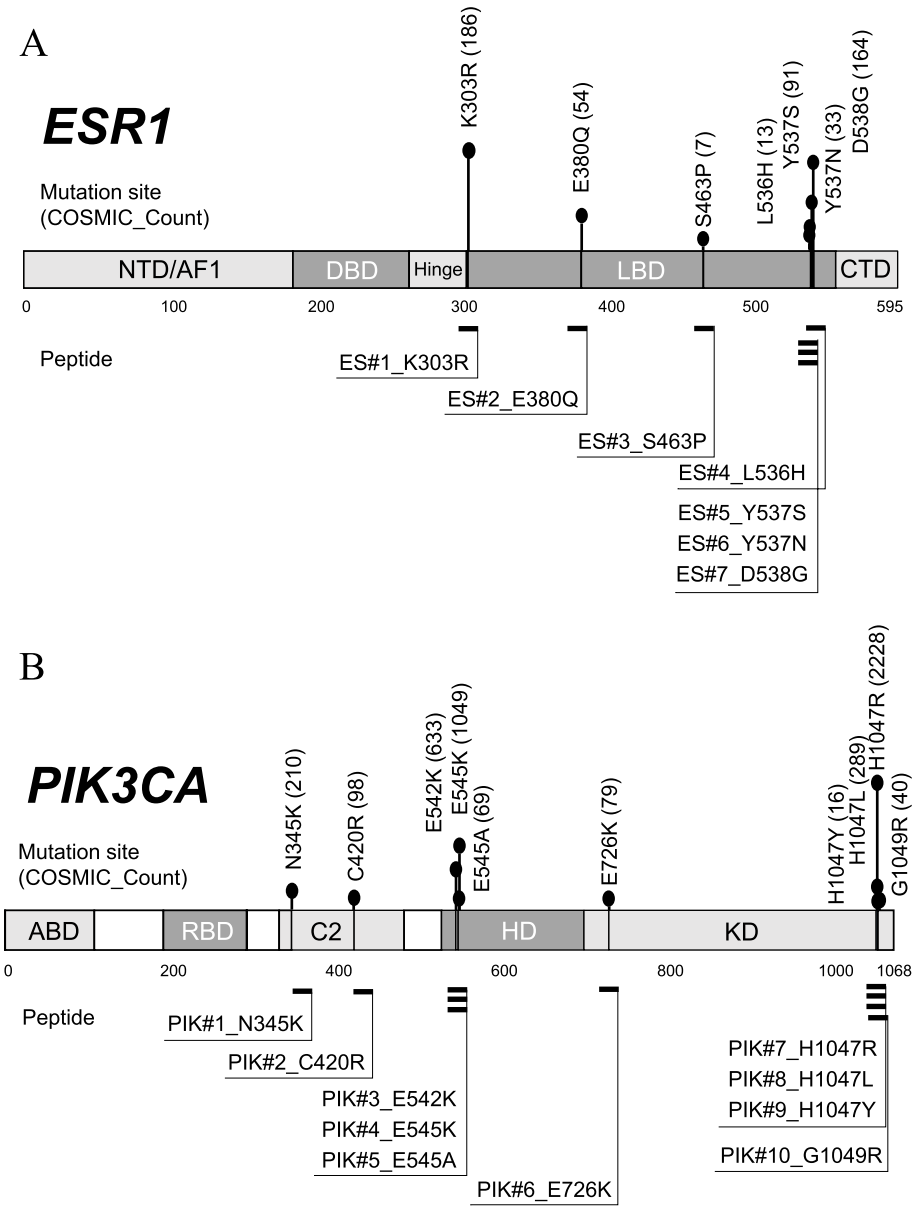

Fig. 1 Overview of *ESR1* and *PIK3CA* mutation sites used in this study. **A**, **B** Positions and COSMIC_Count of mutations in *ESR1* (**A**) and *PIK3CA* (**B**) reported in the COSMIC database. COSMIC_Count represents the number of reports in the COSMIC database. The positions of the peptides are indicated by the horizontal bars in *ESR1* (**A**) and *PIK3CA* (**B**). NTD/AF1, N-terminal domain/activation function 1; DBD, DNA-binding domain; LBD, ligand-binding domain; and CTD, C-terminal domain (**A**). ABD, adaptor-binding domain; RBD, RAS-binding domain; C2, C2 domain; HD, helical domain; and KD, kinase domain (**B**)

regarded as potential DRB4*01:03-restricted epitopes. The %Rank values for these peptides were < 10, with the exception of ES#2_E380Q (%Rank: 14.9) and PIK#10_G1049R (%Rank: 14.3).

According to the predicted binding register, the mutated residue in the peptide binding pocket is located at position −1 (PIK#3_E542K), position 2 (PIK#1_N345K), position 3 (PIK#6_E726K), position 6 (PIK#4,5_E545K/A), position 9 (ES#2_E380Q, PIK#7–9_H1047R/L/Y), and position 11 (PIK#10_G1049R) in the peptide binding groove (Fig. 4A). In these registers, the mutated residues in PIK#1_N345K, PIK#3_E542K, and PIK#6_E726K are accessible from T cell receptor. Some of the peptides could use registers alternative to those shown in Fig. 4A.

Table 1 ESR1 and PIK3CA peptides analyzed in this study

Peptide	Gene	Amino acid substitution	Peptide sequence[a]	%Rank[b]	
				DRB4 *01:03	A *24:02
ES#1_K303R	ESR1	K303R	WPSPLMIKRSK**R**NSL	25.9	19.8
ES#2_E380Q	ESR1	E380Q	DLTLHDQVHLL**Q**CAW	14.9	6.5
ES#3_S463P	ESR1	S463P	GVYTFL**P**STLKSLEE	65.7	0.0
ES#4_L536H	ESR1	L536H	VVP**H**YDLLLEMLDAH	31.4	0.4
ES#5_Y537S	ESR1	Y537S	CKNVVPL**S**DLLLEML	46.2	2.2
ES#6_Y537N	ESR1	Y537N	CKNVVPL**N**DLLLEML	43.6	2.4
ES#7_D538G	ESR1	D538G	CKNVVPLY**G**LLLEML	62.9	0.4
PIK#1_N345K	PIK3CA	N345K	TYV**K**VNIRDIDKIYV	3.4	10.3
PIK#2_C420R	PIK3CA	C420R	EEH**R**PLAWGNINLFD	53.4	8.5
PIK#3_E542K	PIK3CA	E542K	PLS**K**ITEQEKDFLWS	5.0	10.5
PIK#4_E545K	PIK3CA	E545K	PLSEIT**K**QEKDFLWS	3.9	3.4
PIK#5_E545A	PIK3CA	E545A	PLSEIT**A**QEKDFLWS	2.7	1.7
PIK#6_E726K	PIK3CA	E726K	LTDILKQEKKD**K**TQK	1.8	45.5
PIK#7_H1047R	PIK3CA	H1047R	LEYFMKQMNDA**R**HGG	3.4	34.0
PIK#8_H1047L	PIK3CA	H1047L	LEYFMKQMNDA**L**HGG	3.0	7.1
PIK#9_H1047Y	PIK3CA	H1047Y	LEYFMKQMNDA**Y**HGG	3.5	8.8
PIK#10_G1049R	PIK3CA	G1049R	YFMKQMNDAHH**R**GWT	14.3	5.6

[a] Mutant amino acids are bold

[b] Predicted by NetMHCIIpan-4.1 (DRB4*01:03) and NetMHCpan-4.1 (A*24:02)

ES#5–7_Y537S/N, D538G were potentially restricted by DP5, given the high g15 ratio (2.1–3.7) and presence of the DP5 anchor motif [50] (Figure S1). Besides, DP5 was the only allele, in addition to DRB4*01:03, that was shared among ELISPOT-positive donors (donors 2, 3, and 4) (Table S3, S6). However, DP5 was predicted as a non-binder by NetMHCIIpan-4.1 (%Rank 48.7–55.0). An inconsistency between the g15 ratio and %Rank for these peptides was also observed for DRB1*12:01, but not for DRB1*04:05 or DRB1*15:01 (Figure S2). The positive ELISPOT responses for ES#5–7_Y537S/N, D538G, detected in the DP5-negative donor (donor 1), indicated that these peptides can be presented by HLA II other than DP5 in donor 1 (Table S6).

The T cells stimulated with ES#5_Y537S mainly consisted of CD4 + T cells (Figure S3A), whereas T cells stimulated by ES#6_Y537N and ES#7_D538G contained CD8 + T cells (3.8–11.8%) in addition to CD4 + T cells (Figure S3B, C), possibly because of the incomplete depletion of CD8 + T cells before co-culture and their expansion in the presence of IL-2 and peptides. The HLA I allele (HLA-A*02:07) carried by donor 3 was predicted to bind ES#6_Y537N and ES#7_D538G (%Rank; 0.58 and 0.45, respectively), indicating that these peptides are recognized by both CD4 + and CD8 + T cells. This finding is consistent with a previous report that detected ESR1 (Y537S/N and D538G)-specific CD8 + T cells in HLA-A2 positive healthy donors [24].

Potential restriction of ESR1 and PIK3CA mutations by other DR and DP alleles

The alleles that restrict ES#1_K303R were not identified in this study because of the small sample size and absence of anchor motifs for DRB4*01:03 and DP5. ES#3_wt, S463P was presumably restricted by DPA1*01:03-DPB1*02:02 (DP2), which was shared by

(See figure on next page.)

Fig. 2 Summary of the binding prediction and measurement of DRB4*01:03 and DP5. **A** The %Rank predicted by NetMHCIIpan-4.1 and g15 ratio measured by the MHC-density assay for mutant and wt peptides. %Rank < 10 is highlighted in yellow. The g15 ratio > 2.0 is highlighted in light blue. **B**, **C** The g15 ratio for ESR1 (**B**) and PIK3CA peptides (**C**) for DRB4*01:03. **D**, **E** The g15 ratio for ESR1 (**D**) and PIK3CA peptides (**E**) for DP5. The g15 ratio indicates a fold increase in MHC-peptide expression relative to the negative control peptide g15. Data of the g15 ratio < 1.0 are not displayed. In B–E, data for wt (white) and mutant (mut) (gray) (mean ± SD). The red horizontal lines indicate the threshold for a strong binder (g15 ratio = 2.0). Asterisks indicate significant differences between the wt and mutant peptides (*: $p < 0.05$, **: $p < 0.01$, *t*-test)

A

Peptide	DRB4*01:03				DP5			
	Rank		g15 ratio		Rank		g15 ratio	
	wt	mutant	wt	mutant	wt	mutant	wt	mutant
ES#1_K303R	29.7	25.9	1.4	2.1	27.0	27.0	1.0	1.2
ES#2_E380Q	36.4	14.9	<1.0	2.3	83.4	82.6	<1.0	<1.0
ES#3_S463P	56.0	65.7	1.6	1.8	6.1	5.1	2.4	4.0
ES#4_L536H	34.8	31.4	<1.0	1.9	55.6	38.6	4.0	4.9
ES#5_Y537S	62.0	46.2	<1.0	<1.0	66.5	55.0	4.5	3.4
ES#6_Y537N	62.0	43.6	<1.0	<1.0	66.5	49.2	4.5	3.7
ES#7_D538G	62.0	62.9	<1.0	<1.0	66.5	48.7	4.5	2.1
PIK#1_N345K	4.3	3.4	5.0	3.3	47.3	39.4	<1.0	<1.0
PIK#2_C420R	89.2	53.4	1.1	1.8	89.5	55.1	<1.0	1.7
PIK#3_E542K	5.4	5.0	5.7	8.6	54.4	37.1	1.1	1.2
PIK#4_E545K	5.4	3.9	5.7	6.5	54.4	47.6	1.1	1.2
PIK#5_E545A	5.4	2.7	5.7	6.7	54.4	34.5	1.1	1.4
PIK#6_E726K	1.7	1.8	2.1	1.5	19.1	10.9	1.4	1.2
PIK#7_H1047R	1.3	3.4	6.5	4.8	53.6	16.1	1.5	1.4
PIK#8_H1047L	1.3	3.0	6.5	5.0	53.6	48.6	1.5	1.2
PIK#9_H1047Y	1.3	3.5	6.5	3.4	53.6	58.0	1.5	1.4
PIK#10_G1049R	19.7	14.3	9.5	8.7	70.9	51.2	1.9	1.6

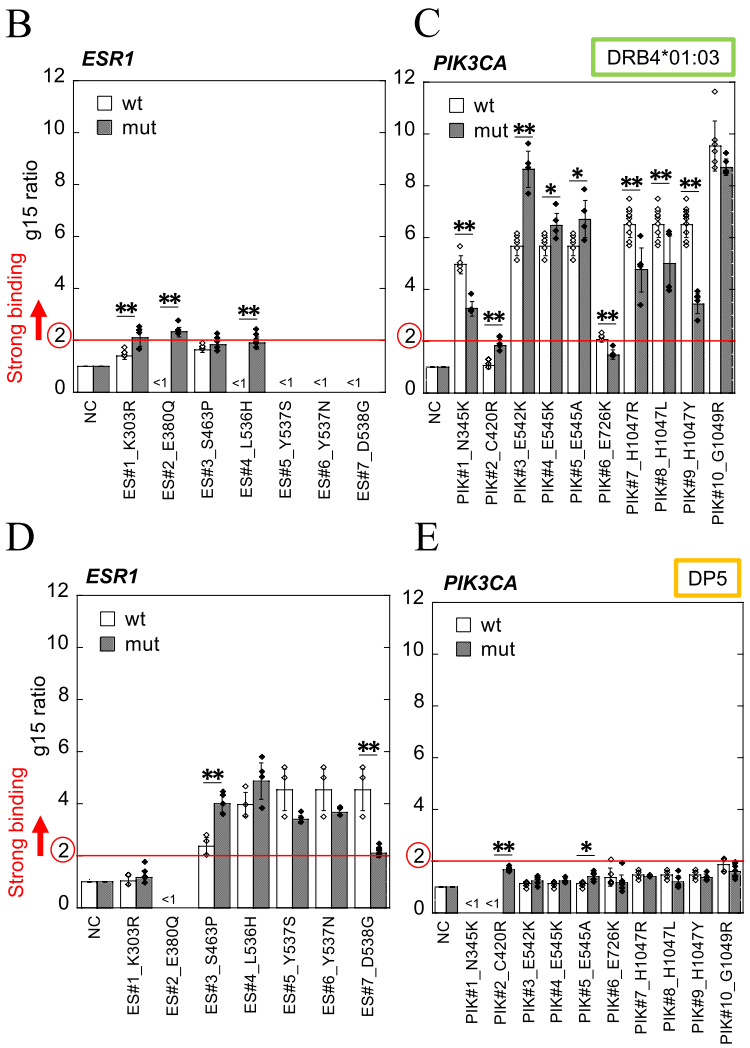

Fig. 2 (See legend on previous page.)

A

ES#2_E380Q

donor (exp)	1 (2)	1 (3)	1 (4)	1 (5)	1 (6)	4	6
NC	0	0	0	0	0	38	47
mutant	4	66	123	336	176	271	TNTC

PIK#5_E545A

donor (exp)	1 (5)	4	6
NC	0	38	47
mutant	364	314	TNTC

PIK#8_H1047L

donor (exp)	1 (1)	1 (2)	1 (4)	1 (5)	4	8
NC	0	0	0	0	38	15
mutant	18	33	28	544	TNTC	34

PIK#9_H1047Y

donor (exp)	1 (1)	1 (2)	1 (3)	1 (4)	3	4	6	7
NC	0	0	0	0	5	38	47	39
mutant	17	18	217	286	49	303	TNTC	98

B

DRB4*01:03 carrier

Number of ELISPOT assays positive responses / total number of assay (range of spot counts)

	DRB1										
	04:05 04:10	04:05 15:01	04:03 09:01	04:05 12:02	09:01 15:02	04:10 14:01	09:01 12:01	04:03 08:03			
	DRB4*01:03										
donor	1	2	3	4	5	6	7	8	penetrance	% Rank	g15 ratio
ES#1_wt	0/6	0/1	0/1	1/1(277)	NA	NA	NA	NA	1/4	29.7	1.4
ES#1_K303R	4/7(4–48)	0/1	0/1	1/1(253)	NA	NA	NA	NA	2/4	25.9	2.1
ES#2_wt	1/6(48)	0/1	1/1(40)	1/1(TNTC)	0/1	0/1	NA	NA	3/6	36.4	<1.0
ES#2_E380Q	5/7(4–336)	0/1	0/1	1/1(271)	1/1(TNTC)	1/1(TNTC)	NA	NA	4/6	14.9	2.3
PIK#1_wt	2/6(8–105)	0/1	0/1	1/1(TNTC)	0/1	1/1(174)	NA	NA	3/6	4.3	5.0
PIK#1_N345K	4/7(19–227)	0/1	0/1	1/1(417)	0/1	0/1	NA	NA	2/6	3.4	3.3
PIK#3–5_wt	0/6	0/1	0/1	1/1(208)	0/1	1/1(239)	NA	NA	2/6	5.4	5.7
PIK#3_E542K	2/7(31–89)	0/1	0/1	1/1(354)	0/1	1/1(247)	NA	NA	3/6	5.0	8.6
PIK#4_E545K	2/6(11–33)	0/1	0/1	1/1(309)	0/1	NA	NA	NA	2/5	3.9	6.5
PIK#5_E545A	1/6(377)	0/1	0/1	1/1(314)	1/1(TNTC)	1/1(TNTC)	NA	NA	4/6	2.7	6.7
PIK#6_wt	0/2	0/1	0/1	1/1(234)	NA	NA	NA	NA	1/4	1.7	2.1
PIK#6_E726K	1/2(63)	0/1	0/1	1/1(201)	NA	NA	NA	NA	2/4	1.8	1.5
PIK#7–9_wt	6/6(7–442)	0/1	0/1	1/1(TNTC)	0/1	1/1(247)	1/1(224)	0/1	4/8	1.3	6.5
PIK#7_H1047R	0/6	0/1	0/1	1/1(317)	0/1	1/1(TNTC)	1/1(143)	0/1	3/8	3.4	4.8
PIK#8_H1047L	4/6(18–558)	0/1	0/1	1/1(TNTC)	1/1(TNTC)	0/1	0/1	1/1(34)	4/8	3.0	5.0
PIK#9_H1047Y	4/7(17–286)	0/1	1/1(46)	1/1(303)	0/1	1/1(TNTC)	1/1(98)	0/1	5/8	3.5	3.4
PIK#10_wt	3/6(16–57)	0/1	0/1	1/1(326)	0/1	NA	NA	NA	2/5	19.7	9.5
PIK#10_G1049R	6/7(8–TNTC)	0/1	0/1	1/1(340)	0/1	1/1(281)	NA	NA	3/6	14.3	8.7

C

DP5 carrier

	DP5					
donor	2	3	4	penetrance	% Rank	g15 ratio
ES#5–7_wt	0/1	0/1	1/1(208)	1/3	66.5	4.5
ES#5_Y537S	1/1(34)	0/1	1/1(316)	2/3	55.0	3.4
ES#6_Y537N	0/1	1/1(37)	1/1(138)	2/3	49.2	3.7
ES#7_D538G	0/1	1/1(124)	1/1(TNTC)	2/3	48.7	2.1

ELISPOT positive (spot counts)
Not analyzed (NA)
%Rank <10
g15 ratio >2.0
TNTC: too numerous to count

Fig. 3 Summary of the ELISPOT assay of healthy donors. **A** Representative data of the ELISPOT assay for ES#2_E380Q, PIK#5_E545A, PIK#8_H1047L, and PIK#9_H1047Y, measured by IFN-γ (red spots) and IL-2 (blue spots). The numbers denote the spot count for IFN-γ (red). NC, negative control. TNTC: too numerous to count. **B**, **C** The ELISPOT profiles for DRB4*01:03 positive donors (**B**) and DP5 positive donors (**C**). The data for peptide pairs that showed penetrance ≥ 0.4 and g15 ratio > 2.0 are presented. HLA alleles of each donor are displayed on the top. Positive ELISPOT responses (IFN-γ) are highlighted in red. Numbers indicate the positive responses/total number of experiments (range of spot counts). The penetrance represents the number of positive donors/numbers of total donors (in red letters). The peptides with %Rank < 10 (NetMHCIIpan-4.1) is highlighted in yellow, and those with a g15 ratio > 2.0 (MHC-density assay) is highlighted in light blue. NA: not analyzed (shadowed in gray). TNTC: too numerous to count

ELISPOT-positive donors (donors 1 and 2) (Table S6). ES#3_wt, S463P peptides were predicted to bind strongly to DP2 (%Rank 1.4–2.3) and contain an anchor motif for DP2 [42, 50]. Similarly, ES#4_L536H was presumably restricted by DRB1*04:05, which was shared by ELISPOT-positive donors (donors 1 and 2). ES#4_L536H was predicted to contain an anchor motif for DRB1*04:05 (Fig. 4B) and bind strongly to DRB1*04:05 (g15 ratio: 2.7–5.3; %Rank: 9.7–18.8) (Table S6).

Among the DRB4*01:03-restricted peptides, PIK#7–9_H1047R/L/Y also contained binding motifs shared by DRB1*04 alleles (P1 (Phe, Tyr, Leu, and Ile) and P6 (Thr, Asn, Asp, and Ser)) (Fig. 4B, C). Some ELISPOT-positive donors for PIK#7–9_H1047R/L/Y (donors 1, 3, 4, 6, and 8) carried these DRB1*04 alleles (DRB1*04:03, *04:05, or *04:10) (Table S7). The g15 ratios of PIK#7–9_H1047R/L/Y for DRB1*04:01 and DRB1*04:05 were 1.9 to 4.2 (Table S8), and the %Rank values for other DRB1*04 alleles were 1.9 to 9.1 (Table S9). From these data, we inferred that PIK#7–9_H1047R/L/Y can be presented by DRB1*04:03, DRB1*04:05, and DRB1*04:10, in addition to DRB4*01:03.

HLA II of the donors used in the ELISPOT assay were skewed toward alleles frequently found in East Asian populations. To elucidate the presentation of hot spot mutations on alleles commonly found in global populations, we extended the MHC-density assay to include additional DRB1 alleles that are not present in donors 1–8. For ESR1, a g15 ratio > 2.0 was achieved by DRB1*01:01 (ES#6_Y537N) and DRB1*15:01 (ES#5–6_wt, Y537S/N)

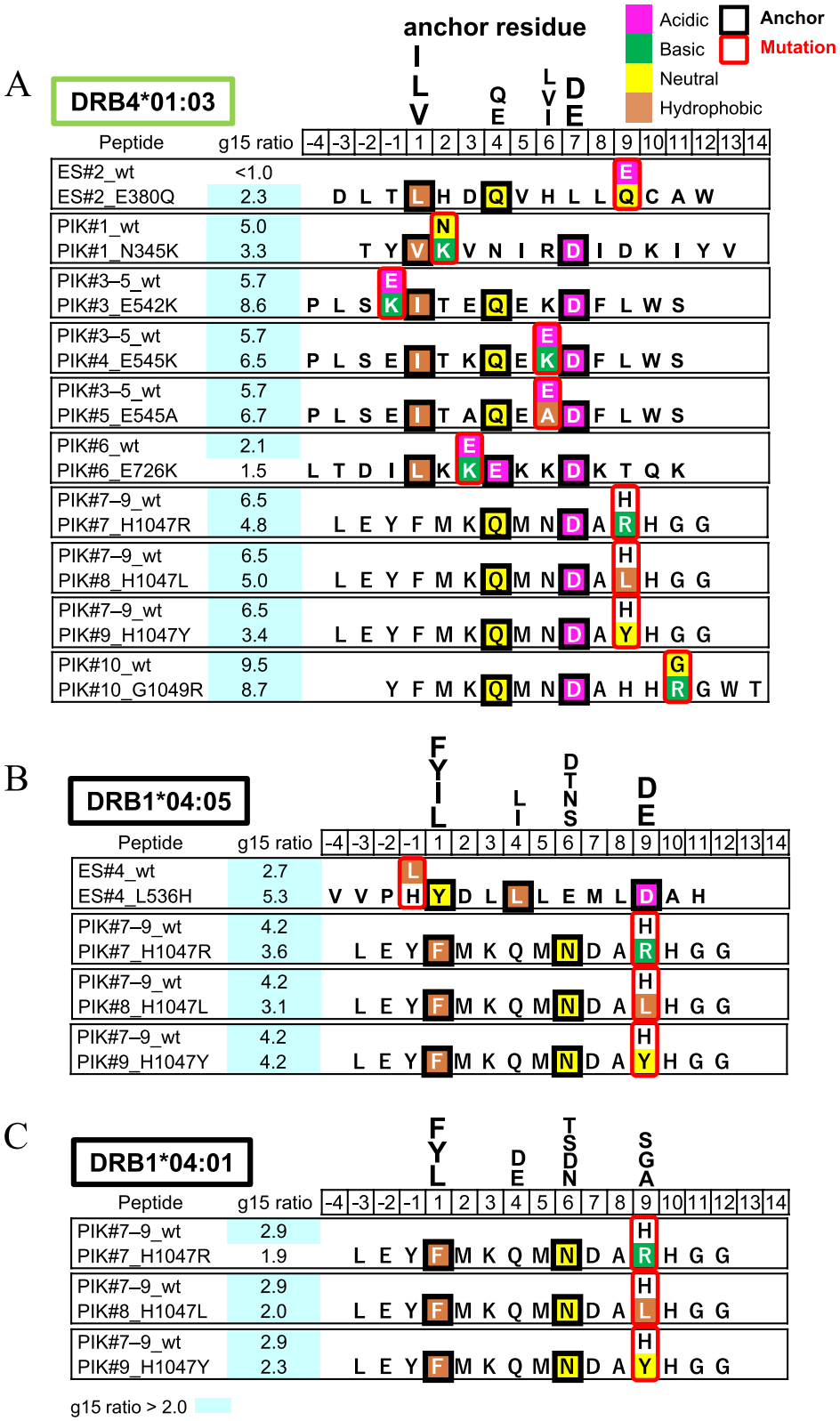

Fig. 4 Possible binding registers of ESR1- and PIK3CA-peptides. **A**-**C** Binding registers of peptides, inferred from known anchor residues for DRB4*01:03 (**A**), DRB1*04:05 (**B**), and DRB1*04:01 (**C**). The peptides with a g15 ratio > 2.0 are highlighted in light blue. Anchor residues (boxed in black) and the mutation sites (boxed in red). The amino acids are color-coded: acidic (pink), basic (green), neutral (yellow), or hydrophobic (brown)

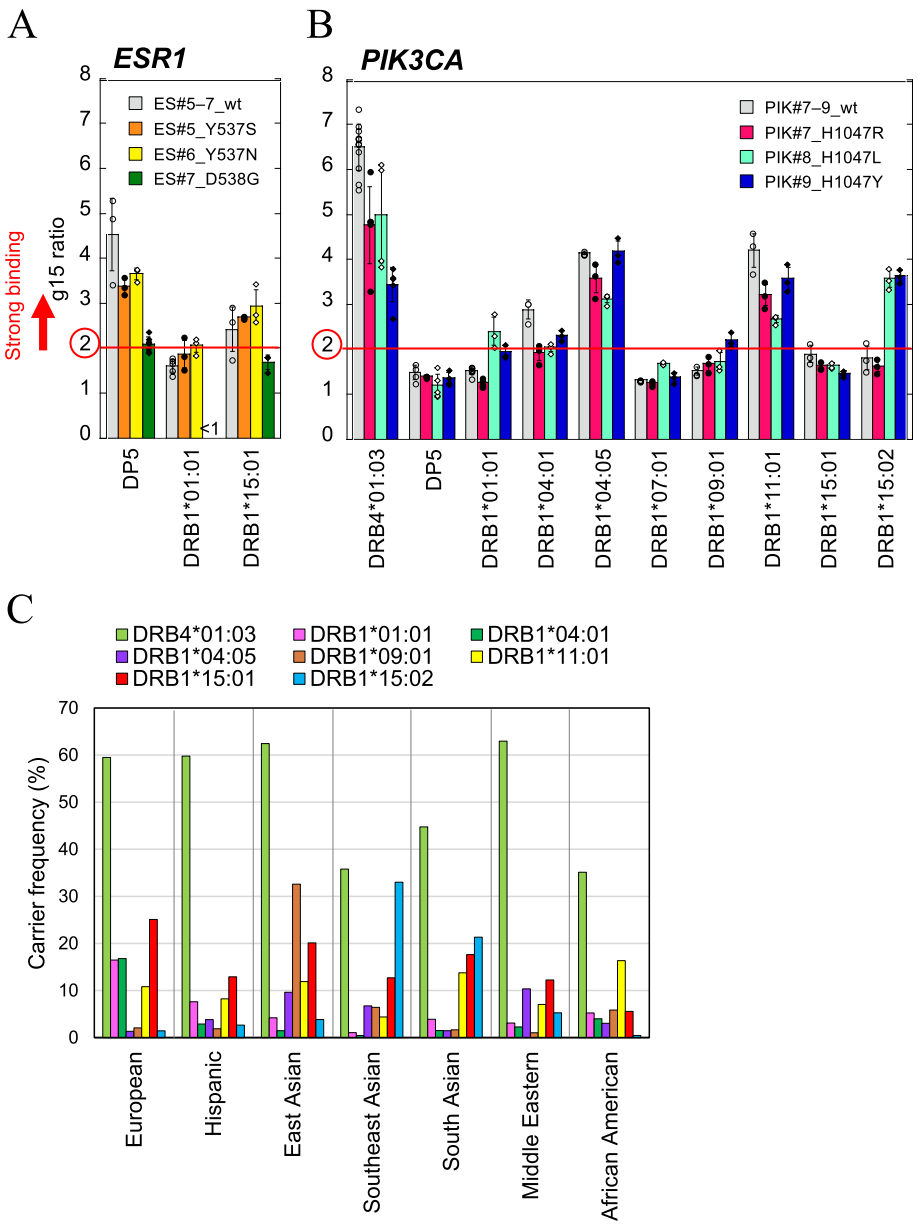

Fig. 5 The g15 ratio measured for various DRB1 alleles. **A**, **B** The g15 ratios for ES#5–7_wt (gray) and ES#5_Y537S (orange), ES#6_Y537N (yellow) and ES#7_D538G (green) (**A**) and for PIK#7–9_wt (gray), PIK#7_H1047R (red), PIK#8_H1047L (light blue), and PIK#9_H1047Y (dark blue) (mean ± SD) (**B**). The red horizontal line indicates the threshold for a strong binder (g15 ratio = 2.0). **C** Carrier frequency of the DRB4*01:03 and DRB1 alleles analyzed in (**A**) and (**B**). The frequencies are based on allelefrequencies.net (Methods)

(Fig. 5A, Table S8, S10). For PIK#7–9_H1047R/L/Y, a g15 ratio > 2.0 was achieved by DRB1*01:01, DRB1*04:01, DRB1*04:05, DRB1*09:01, DRB1*11:01, and DRB1*15:02 (Fig. 5B, Table S8, S10). PIK#5_E545A, but not the wt peptide, was presented by DRB1*03:01 (g15 ratio: 2.4) (Table S8, S10). These additional DRB1 alleles are frequently found in populations worldwide (Fig. 5C).

Collectively, the presentation of ES#5–7_Y537S/N, D538G, and PIK#7–9_H1047R/L/Y on the major HLA II alleles, in addition to DRB4*01:03 or DP5 (summarized in Table S10), suggests the broad applicability of these mutations, in terms of HLA II restriction, for immunotherapy. However, the binding analysis in this study was limited to the most frequent allele-peptide

pairs. Analysis of a larger cohort of healthy donors or patients is required to further elucidate the HLA II allele specificity for each mutation, as well as to confirm the restriction patterns inferred from binding measurements.

Inconsistency of measured and predicted binding

A comparison of the MHC-density assay and prediction by NetMHCIIpan-4.1 revealed similarities and differences in their binding profiles (Fig. 2A). PIK3CA-peptides that showed ELISPOT positivity and were inferred as DRB4*01:03-restricted epitopes (g15 ratio > 2.0 for DRB4*01:03) were predicted to be strong or weak binders (%Rank < 10), except for ES#2_E380Q and PIK#10_G1049R (%Rank 14.9, and 14.3, respectively) (Fig. 3B). The %Rank for ES#2_E380Q was even larger (%Rank: 17.9) in the latest version of NetMHCIIpan (version 4.3), whereas the rank predicted by the other prediction tool, MixMHC2pred-2.0 [51, 52], was 10.2 (Table S11). The potential DP5-resticted peptides ES#5–7_Y537S/N, D538G (g15 ratio: 2.1–4.5) were predicted to be non-binders by NetMHCII pan-4.1 (%Rank: 48.7–66.5). The %Rank and g15 ratio for ES#5–7_Y537S/N, D538G were consistent for DRB1*04:05 and DRB1*15:01 but not for DRB1*12:01 (Figure S2).

Figure 6A and B show a comparison of the g15 ratio and %Rank for the potential DRB4*01:03-and DP5-restricted peptides. The inconsistency between the measurement and prediction, in terms of the binding hierarchy between wt and mutant peptides, observed for PIK#1_N345K (for DRB4*01:03) and ES#7_D538G (for DP5) (Fig. 6A, B) suggests the difficulty in predicting the influence of mutation on presentation to HLA II.

Discussion

In the present study, we analyzed HLA II presentation and CD4 + T cell responses of hotspot mutations in *ESR1* and *PIK3CA* using PBMCs from healthy donors. Positive IFN-γ responses were detected for 16 peptides that contained some of the most frequent mutations: ESR1 (E380Q), ESR1 (Y537S/N, D538G), PIK3CA (E542K, E545K/A) and PIK3CA (H1047R/L/Y) [53–55]. ESR1 Y537S/N is considered a promising immunotherapy target because it elicits antitumor responses by CD8 + T cells in a murine model [23] and is recognized by CD8 + T cells from healthy donors and patients with breast cancer [23, 24]. Our study revealed that ES#5–7_Y537S/N, D538G are recognized by CD4 + T cells of healthy individuals, possibly through presentation by DP5, as well as DRB1*01:01 and DRB1*15:01 (Figs. 3C, 5A, Table S8, S10).

PIK3CA (H1047R/L/Y) is one of the most frequent hotspot mutations in breast cancer [56] and solid tumors, including uterine/endometrial, cervical, and ovarian tumors [57]. PIK3CA (H1047R/L/Y) elicits antitumor responses by CD8 + T cells in murine xenograft models [25] and in cytotoxic assays [25, 26]. Notably, PIK3CA (H1047R/L/Y) peptides can be presented by DRB4*01:03, which is carried in approximately 35–63% of various populations (Fig. 5C), and by major DRB1 alleles, including DRB1*04:01, DRB1*04:05, DRB1*09:01, DRB1*11:01, and DRB1*15:02 (Table S10). These findings suggest that PIK3CA (H1047R/L/Y) peptides can be presented abundantly in individuals with the DRB1*04:01- or DRB1*04:05-DRB4*01:03 haplotypes.

An important limitation of this study is the use of healthy donors, not patients with breast cancer, for the ELISPOT assay. Owing to the immunosuppressive condition of the tumor microenvironment, the penetrance in the patient cohort could be lower than that observed in healthy donors, as reported for the CD8 + T cell ELISPOT assay for ESR1 Y537S/N/C [24]. Further studies are warranted to confirm the CD4 + T cell responses to ESR1 and PIK3CA mutations, including indels that were not analyzed in this study, in HR + endocrine-resistant breast cancer patients to identify the most targetable sites.

Another limitation was the small number of donors used for the ELISPOT assay. The number of DRB4*01:03-positive donors ($n = 8$) appeared to be sufficient to detect potential DRB4*01:03-restriction, but not other less frequent DRB1 alleles; a larger-scale analysis will be required to confirm their restrictions. The restriction of ES#5–7_Y537S/N, D538G by DP5 should also be interpreted with caution, given the small number of DP5-positive donors and inconsistency between the measurement and prediction (Figure S2).

We found discrepancy between MHC-peptide binding measured by MHC-density assay and prediction. While the g15 ratio was consistent with NetMHCIIpan-4.1 prediction for most peptides, the high g15 ratio (> 2.0) and %Rank below the threshold (%Rank > 10) observed for ES#2_E380Q and PIK#10_G1049R (for DRB4*01:03) and ES#5–7_Y537S/N, D538G (for DP5 and DRB1*12:02) suggested an inconsistency between the measurement and prediction (Figure S2), as reported for HLA I-restricted epitopes in triple-negative breast cancer [58]. This inconsistency may be ascribed to the quality and/or quantity of the training dataset for certain alleles, which remains to be confirmed. The difficulty in fully predicting immunogenic peptides implies that there may be neoantigens not detectable by prediction.

Although the tumor microenvironment of HR + breast cancer makes this subtype a difficult immunotherapy target [5, 59, 60], growing evidence from preclinical models has revealed the recognition of ESR1 (E380Q, Y537S/N/C) and PIK3CA (H1047R/L/Y) mutations

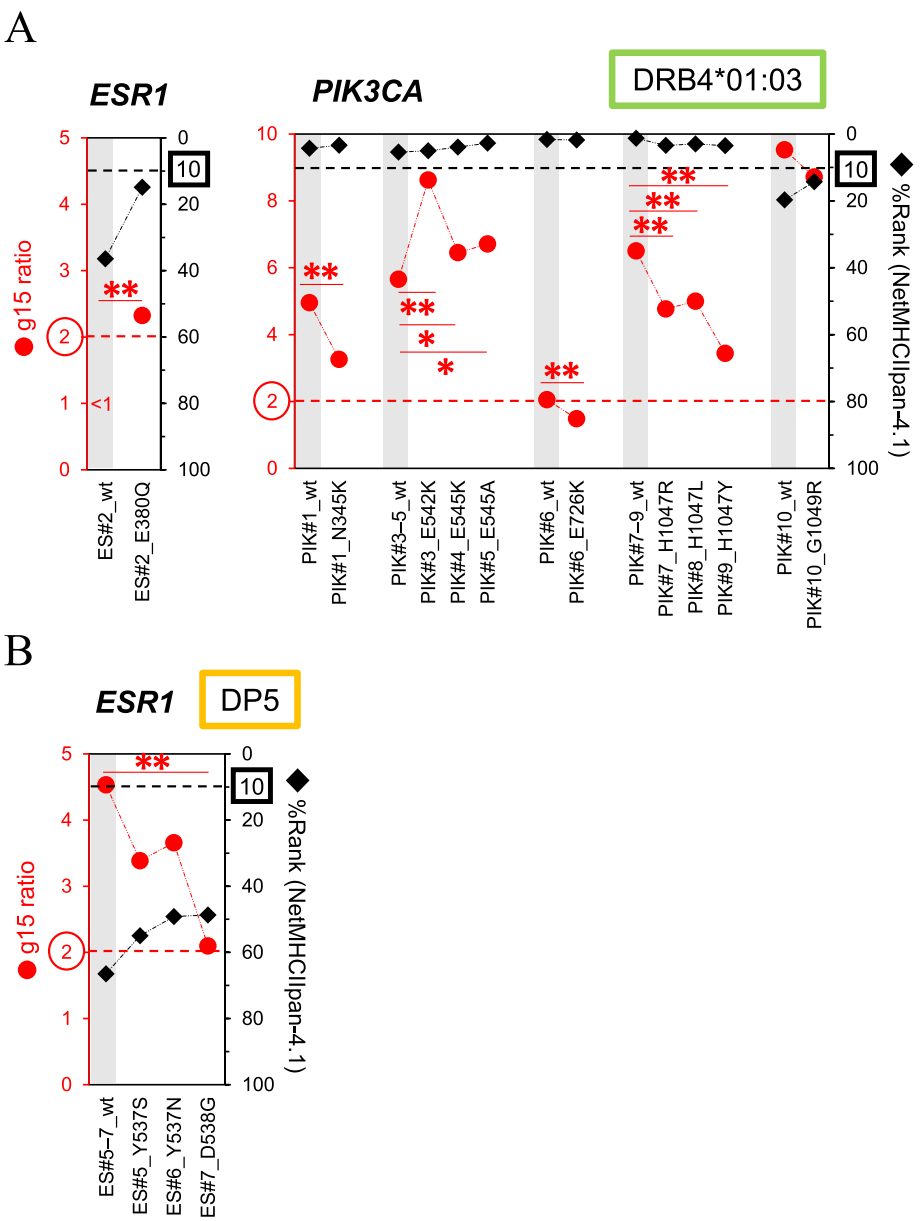

Fig. 6 Comparison of the measured and predicted binding patterns. **A**, **B** g15 ratio and %Rank of DRB4*01:03 for ESR1 (left panel) and PIK3CA peptides (right panel) (**A**) and of DP5 for ESR1 peptides (**B**). The data of g15 ratio < 1.0 are not displayed. The horizontal dot lines (black) denote the threshold (%Rank = 10) for a weak binder predicted by NetMHCIIpan-4.1. The horizontal dot lines (red) denote the threshold for a strong binder (g15 ratio = 2.0) by the MHC-density assay. Asterisks indicate significant differences between the wt and mutant peptides (*: $p < 0.05$, **: $p < 0.01$, *t*-test)

by CD8 + T cells [22, 23, 25, 26]. The potential clinical efficacy of vaccines targeting common driver mutations, including PIK3CA E545K, in renal cell carcinoma [61], demonstrates that key driver mutations can induce antitumor immunity in low TMB cancers. The selective presentation of *ESR1* and *PIK3CA* mutations on common HLA II alleles shown in this study suggests that the HLA II presentation of driver mutations can vary between individuals and supports further systematic analysis to identify favorable HLA types for each mutation, leading to the design of effective multi-epitope vaccines applicable to a broad population.

Conclusions

Our study revealed that public neoantigens in *ESR1* and *PIK3CA* are recognized by CD4+T cells upon the presentation on common HLA II alleles. Further studies are warranted to elucidate the landscape of HLA II presentation and clinical applicability of these mutations in immunotherapy for endocrine-resistant breast cancer.

Abbreviations

COSMIC	Catalog of Somatic Mutations in Cancer
ELISPOT	Enzyme-Linked ImmunoSpot
ERα	Estrogen receptor alpha
ESR1	*Estrogen receptor 1*
FCM	Flow cytometry
g15	15-mer of glycine
GM-CSF	Granulocyte-macrophage colony-stimulating factor
HLA	Human leukocyte antigen
HLA I	HLA class I
HLA II	HLA class II
HR+	Hormone receptor-positive
ICIs	Immune checkpoint inhibitors
IFN-γ	Interferon-gamma
IL-2	Interleukin-2
IL-4	Interleukin-4
mDCs	Mature dendritic cells
MFI	Median fluorescence intensity
MHC	Major histocompatibility complex
mTOR	Mammalian target of rapamycin
mut	Mutant
NA	Not analyzed
PBMC	Peripheral blood mononuclear cell
PI3K	Phosphatidylinositol 3-kinase
PIK3CA	*Phosphatidylinositol-4,5-bisphosphate 3-kinase catalytic subunit alpha*
SD	Standard deviation
Th	T helper
TMB	Tumor mutational burden
TNF-α	Tumor necrosis factor-alpha
TNTC	Too numerous to count
wt	Wild-type

Supplementary Information

The online version contains supplementary material available at https://doi.org/10.1186/s12885-025-13992-6.

Supplementary Material 1: Table S1 *ESR1* mutations reported in the COSMIC database. Table S2 *PIK3CA* mutations reported in the COSMIC database. Table S3 HLA alleles in healthy donors. Table S4 Summary of ELISPOT assays (donor 1). Table S5 Summary of ELISPOT assays (donors 1–8). Table S6 The %Rank, g15 ratio, and immunogenicity of ESR1 peptides. Table S7 The %Rank, g15 ratio, and immunogenicity of PIK3CA peptides. Table S8 Summary of binding prediction and measurement for 13 HLA II alleles. Table S9 %Rank for DRB1*04 alleles. Table S10 List of HLA II alleles (g15 ratio >2.0). Table S11 Comparison of HLA II-peptide binding predictions.

Supplementary Material 2: Figure S1 Possible binding registers of ESR1-peptides. Figure S2 Comparison of measured and predicted binding patterns. Figure S3 Compositions of antigen-specific T cells.

Acknowledgements

We would like to acknowledge the RIKEN Bioresource Center for providing the NIH3T3 cells and Toshio Kitamura (The Institute of Medical Sciences, University of Tokyo) for providing the retroviral vectors. We thank Nian Jiang and Aoi Yanahira for their technical assistance. We are grateful to all the participants in this study.

Authors' contributions

YA: Conceptualization, Data curation, Funding acquisition, Investigation, Methodology, Visualization, Writing - original draft, Writing - review & editing. HM: Conceptualization, Investigation, Methodology, Supervision, Writing - original draft, Writing - review & editing. HB: Funding acquisition, Project administration, Supervision, Writing - review & editing. SH: Conceptualization, Funding acquisition, Project administration, Supervision, Writing - review & editing. EN: Project administration, Supervision, Writing - review & editing. HH: Project administration, Supervision, Writing - review & editing. All authors read and approved the final manuscript.

Funding

This study was funded by JSPS KAKENHI Grant Numbers 21K08614 and 24K11737.

Data availability

All data supporting the findings of this study are available within the paper and its Supplementary Information.

Declarations

Ethics approval and consent to participate

Approval of the Research Protocol: This study was conducted in compliance with the ethical standards of the Helsinki Declaration and its later amendments and approved by the Clinical Research Ethics Review Committee of Tsukuba University Hospital (H29-069).
Informed Consent: Written informed consent was obtained from all participating healthy donors.
Registry and the Registration No. of the study/trial: N/A.
Animal Studies: N/A.

Consent for publication

Not applicable.

Competing interests

H.M. has filed a patent on the MHC density assay.

Received: 18 October 2024 Accepted: 21 March 2025
Published online: 04 April 2025

References

1. Arnold M, Morgan E, Rumgay H, Mafra A, Singh D, Laversanne M, Vignat J, Gralow JR, Cardoso F, Siesling S, et al. Current and future burden of breast cancer: global statistics for 2020 and 2040. Breast. 2022;66:15–23.
2. Howlader N, Altekruse SF, Li CI, Chen VW, Clarke CA, Ries LA, Cronin KA. US incidence of breast cancer subtypes defined by joint hormone receptor and HER2 status. J Natl Cancer Inst 2014;106(5):dju055.
3. Dustin D, Gu G, Fuqua SAW. ESR1 mutations in breast cancer. Cancer. 2019;125(21):3714–28.
4. Narang P, Chen M, Sharma AA, Anderson KS, Wilson MA. The neoepitope landscape of breast cancer: implications for immunotherapy. BMC Cancer. 2019;19(1):200.
5. Goldberg J, Pastorello RG, Vallius T, Davis J, Cui YX, Agudo J, Waks AG, Keenan T, McAllister SS, Tolaney SM, et al. The immunology of hormone receptor positive breast cancer. Front Immunol. 2021;12: 674192.
6. Jardim DL, Goodman A, de Melo GD, Kurzrock R. The challenges of tumor mutational burden as an immunotherapy biomarker. Cancer Cell. 2021;39(2):154–73.
7. Weber JS, Carlino MS, Khattak A, Meniawy T, Ansstas G, Taylor MH, Kim KB, McKean M, Long GV, Sullivan RJ, et al. Individualised neoantigen therapy mRNA-4157 (V940) plus pembrolizumab versus pembrolizumab monotherapy in resected melanoma (KEYNOTE-942): a randomised, phase 2b study. Lancet. 2024;403(10427):632–44.
8. Rojas LA, Sethna Z, Soares KC, Olcese C, Pang N, Patterson E, Lihm J, Ceglia N, Guasp P, Chu A, et al. Personalized RNA neoantigen vaccines stimulate T cells in pancreatic cancer. Nature. 2023;618(7963):144–50.

9. Khattak A, Weber JS, Meniawy T, Taylor MH, Ansstas G, Kim KB, McKean M, Long GV, Sullivan RJ, Faries MB et al.: Distant metastasis-free survival results from the randomized, phase 2 mRNA-4157-P201/KEYNOTE-942 trial. J Clin Oncol. 2023, 41(17_suppl):LBA9503-LBA9503.
10. Priestley P, Baber J, Lolkema MP, Steeghs N, de Bruijn E, Shale C, Duyvesteyn K, Haidari S, van Hoeck A, Onstenk W, et al. Pan-cancer whole-genome analyses of metastatic solid tumours. Nature. 2019;575(7781):210–6.
11. Irani S, Tan W, Li Q, Toy W, Jones C, Gadiya M, Marra A, Katzenellenbogen JA, Carlson KE, Katzenellenbogen BS, et al. Somatic estrogen receptor alpha mutations that induce dimerization promote receptor activity and breast cancer proliferation. J Clin Invest. 2024;134(1):e163242.
12. Drouyer A, Beaussire L, Jorda P, Leheurteur M, Guillemet C, Berghian A, Georgescu D, Di Fiore F, Perdrix A, Clatot F. Clinical relevance of circulating ESR1 mutations during endocrine therapy for advanced hormone-dependent endometrial carcinoma. BMC Cancer. 2023;23(1):1061.
13. Dessources K, Miller KM, Kertowidjojo E, Da Cruz Paula A, Zou Y, Selenica P, da Silva EM, Benayed R, Ashley CW, Abu-Rustum NR, et al. ESR1 hotspot mutations in endometrial stromal sarcoma with high-grade transformation and endocrine treatment. Mod Pathol. 2022;35(7):972–8.
14. Barone I, Iacopetta D, Covington KR, Cui Y, Tsimelzon A, Beyer A, Ando S, Fuqua SA. Phosphorylation of the mutant K303R estrogen receptor alpha at serine 305 affects aromatase inhibitor sensitivity. Oncogene. 2010;29(16):2404–14.
15. Keraite I, Alvarez-Garcia V, Garcia-Murillas I, Beaney M, Turner NC, Bartos C, Oikonomidou O, Kersaudy-Kerhoas M, Leslie NR. PIK3CA mutation enrichment and quantitation from blood and tissue. Sci Rep. 2020;10(1):17082.
16. Mankoo PK, Sukumar S, Karchin R. PIK3CA somatic mutations in breast cancer: mechanistic insights from Langevin dynamics simulations. Proteins. 2009;75(2):499–508.
17. Janku F, Tsimberidou AM, Garrido-Laguna I, Wang X, Luthra R, Hong DS, Naing A, Falchook GS, Moroney JW, Piha-Paul SA, et al. PIK3CA mutations in patients with advanced cancers treated with PI3K/AKT/mTOR axis inhibitors. Mol Cancer Ther. 2011;10(3):558–65.
18. Vasan N, Razavi P, Johnson JL, Shao H, Shah H, Antoine A, Ladewig E, Gorelick A, Lin TY, Toska E, et al. Double PIK3CA mutations in cis increase oncogenicity and sensitivity to PI3Kalpha inhibitors. Science. 2019;366(6466):714–23.
19. Li Z, McGinn O, Wu Y, Bahreini A, Priedigkeit NM, Ding K, Onkar S, Lampenfeld C, Sartorius CA, Miller L, et al. ESR1 mutant breast cancers show elevated basal cytokeratins and immune activation. Nat Commun. 2022;13(1):2011.
20. Skriver SK, Jensen MB, Knoop AS, Ejlertsen B, Laenkholm AV. Tumour-infiltrating lymphocytes and response to neoadjuvant letrozole in patients with early oestrogen receptor-positive breast cancer: analysis from a nationwide phase II DBCG trial. Breast Cancer Res. 2020;22(1):46.
21. Sobral-Leite M, Salomon I, Opdam M, Kruger DT, Beelen KJ, van der Noort V, van Vlierberghe RLP, Blok EJ, Giardiello D, Sanders J, et al. Cancer-immune interactions in ER-positive breast cancers: PI3K pathway alterations and tumor-infiltrating lymphocytes. Breast Cancer Res. 2019;21(1):90.
22. Goldberg J, Qiao N, Guerriero JL, Gross B, Meneksedag Y, Lu YF, Philips AV, Rahman T, Meric-Bernstam F, Roszik J, et al. Estrogen receptor mutations as novel targets for immunotherapy in metastatic estrogen receptor-positive breast cancer. Cancer Res Commun. 2024;4(2):496–504.
23. Dailey GP, Rabiola CA, Lei G, Wei J, Yang XY, Wang T, Liu CX, Gajda M, Hobeika AC, Summers A, et al. Vaccines targeting ESR1 activating mutations elicit anti-tumor immune responses and suppress estrogen signaling in therapy resistant ER+ breast cancer. Hum Vaccin Immunother. 2024;20(1): 2309693.
24. Lopez M, Spehner L, André F, Viot J, Seffar E, Marguier A, Curtit E, Meynard G, Dobi E, Ladoire S, et al. Exploring the role of ESR1 mutations in metastatic hormone receptor-positive breast cancer T cell immune surveillance disruption. Breast Cancer Res. 2025;27(1):19.
25. Chandran SS, Ma J, Klatt MG, Dundar F, Bandlamudi C, Razavi P, Wen HY, Weigelt B, Zumbo P, Fu SN, et al. Immunogenicity and therapeutic targeting of a public neoantigen derived from mutated PIK3CA. Nat Med. 2022;28(5):946–57.
26. Shen M, Chen S, Han X, Hao Y, Wang J, Li L, Chen T, Wang B, Zou L, Zhang T, et al. Identification of an HLA-A*11:01-restricted neoepitope of mutant PIK3CA and its specific T cell receptors for cancer immunotherapy targeting hotspot driver mutations. Cancer Immunol Immunother. 2024;73(8):150.
27. Lam N, Lee Y, Farber DL. A guide to adaptive immune memory. Nat Rev Immunol. 2024;24(11):810–29.
28. Borst J, Ahrends T, Babala N, Melief CJM, Kastenmuller W. CD4(+) T cell help in cancer immunology and immunotherapy. Nat Rev Immunol. 2018;18(10):635–47.
29. Yossef R, Tran E, Deniger DC, Gros A, Pasetto A, Parkhurst MR, Gartner JJ, Prickett TD, Cafri G, Robbins PF, et al. Enhanced detection of neoantigen-reactive T cells targeting unique and shared oncogenes for personalized cancer immunotherapy. JCI Insight. 2018;3(19):e122467.
30. Kreiter S, Vormehr M, van de Roemer N, Diken M, Lower M, Diekmann J, Boegel S, Schrors B, Vascotto F, Castle JC, et al. Mutant MHC class II epitopes drive therapeutic immune responses to cancer. Nature. 2015;520(7549):692–6.
31. Alspach E, Lussier DM, Miceli AP, Kizhvatov I, DuPage M, Luoma AM, Meng W, Lichti CF, Esaulova E, Vomund AN, et al. MHC-II neoantigens shape tumour immunity and response to immunotherapy. Nature. 2019;574(7780):696–701.
32. Brightman SE, Naradikian MS, Miller AM, Schoenberger SP. Harnessing neoantigen specific CD4 T cells for cancer immunotherapy. J Leukoc Biol. 2020;107(4):625–33.
33. Ward JP, Gubin MM, Schreiber RD. The role of neoantigens in naturally occurring and therapeutically induced immune responses to cancer. Adv Immunol. 2016;130:25–74.
34. van der Burg SH, Arens R, Ossendorp F, van Hall T, Melief CJ. Vaccines for established cancer: overcoming the challenges posed by immune evasion. Nat Rev Cancer. 2016;16(4):219–33.
35. Solinas C, Aiello M, Migliori E, Willard-Gallo K, Emens LA. Breast cancer vaccines: heeding the lessons of the past to guide a path forward. Cancer Treat Rev. 2020;84:101947.
36. Hirata-Nozaki Y, Ohkuri T, Ohara K, Kumai T, Nagata M, Harabuchi S, Kosaka A, Nagato T, Ishibashi K, Oikawa K, et al. PD-L1-specific helper T-cells exhibit effective antitumor responses: new strategy of cancer immunotherapy targeting PD-L1 in head and neck squamous cell carcinoma. J Transl Med. 2019;17(1):207.
37. Hirayama M, Nishimura Y. The present status and future prospects of peptide-based cancer vaccines. Int Immunol. 2016;28(7):319–28.
38. Sondka Z, Dhir NB, Carvalho-Silva D, Jupe S, Madhumita N, McLaren K, Starkey M, Ward S, Wilding J, Ahmed M, et al. COSMIC: a curated database of somatic variants and clinical data for cancer. Nucleic Acids Res. 2024;52(D1):D1210–7.
39. Naruse TK, Ando R, Nose Y, Kagiya M, Ando H, Kawata H, Nabeya N, Isshiki G, Inoko H. HLA-DRB4 genotyping by PCR-RFLP: diversity in the associations between HLA-DRB4 and DRB1 alleles. Tissue Antigens. 1997;49(2):152–9.
40. Nakajima F, Nakamura J, Yokota T. Analysis of HLA haplotypes in Japanese, using high resolution allele typing. Major Histocompatibility Complex. 2001;8(1):1–32.
41. Gonzalez-Galarza FF, McCabe A, Santos E, Jones J, Takeshita L, Ortega-Rivera ND, Cid-Pavon GMD, Ramsbottom K, Ghattaoraya G, Alfirevic A, et al. Allele frequency net database (AFND) 2020 update: gold-standard data classification, open access genotype data and new query tools. Nucleic Acids Res. 2020;48(D1):D783–8.
42. Reynisson B, Barra C, Kaabinejadian S, Hildebrand WH, Peters B, Nielsen M. Improved prediction of MHC II antigen presentation through integration and motif deconvolution of mass spectrometry MHC eluted ligand data. J Proteome Res. 2020;19(6):2304–15.
43. Jurtz V, Paul S, Andreatta M, Marcatili P, Peters B, Nielsen M. NetMHCpan-4.0: improved peptide-MHC class I interaction predictions integrating eluted ligand and peptide binding affinity data. J Immunol. 2017;199(9):3360–8.
44. Sakai K, Miyadera H, Kubo M, Nakajima F, Matsumoto M. Overlapping ADAMTS13 peptide binding profiles of DRB1 *08:03 and DRB1 *11:01 suggest a common etiology of immune-mediated thrombotic thrombocytopenic purpura. J Thromb Haemost. 2023;21(3):616–28.
45. Kitamura T, Koshino Y, Shibata F, Oki T, Nakajima H, Nosaka T, Kumagai H. Retrovirus-mediated gene transfer and expression cloning: powerful tools in functional genomics. Exp Hematol. 2003;31(11):1007–14.
46. Morita S, Kojima T, Kitamura T. Plat-E: an efficient and stable system for transient packaging of retroviruses. Gene Ther. 2000;7(12):1063–6.

47. Miyadera H, Ohashi J, Lernmark A, Kitamura T, Tokunaga K. Cell-surface MHC density profiling reveals instability of autoimmunity-associated HLA. J Clin Invest. 2015;125(1):275–91.
48. Moodie Z, Price L, Gouttefangeas C, Mander A, Janetzki S, Lower M, Welters MJ, Ottensmeier C, van der Burg SH, Britten CM. Response definition criteria for ELISPOT assays revisited. Cancer Immunol Immunother. 2010;59(10):1489–501.
49. Boulet S, Ndongala ML, Peretz Y, Boisvert MP, Boulassel MR, Tremblay C, Routy JP, Sekaly RP, Bernard NF. A dual color ELISPOT method for the simultaneous detection of IL-2 and IFN-gamma HIV-specific immune responses. J Immunol Methods. 2007;320(1–2):18–29.
50. Kusano S, Kukimoto-Niino M, Satta Y, Ohsawa N, Uchikubo-Kamo T, Wakiyama M, Ikeda M, Terada T, Yamamoto K, Nishimura Y, et al. Structural basis for the specific recognition of the major antigenic peptide from the Japanese cedar pollen allergen Cry j 1 by HLA-DP5. J Mol Biol. 2014;426(17):3016–27.
51. Racle J, Guillaume P, Schmidt J, Michaux J, Larabi A, Lau K, Perez MAS, Croce G, Genolet R, Coukos G, et al. Machine learning predictions of MHC-II specificities reveal alternative binding mode of class II epitopes. Immunity. 2023;56(6):1359-1375 e1313.
52. Racle J, Michaux J, Rockinger GA, Arnaud M, Bobisse S, Chong C, Guillaume P, Coukos G, Harari A, Jandus C, et al. Robust prediction of HLA class II epitopes by deep motif deconvolution of immunopeptidomes. Nat Biotechnol. 2019;37(11):1283–6.
53. Fribbens C, O'Leary B, Kilburn L, Hrebien S, Garcia-Murillas I, Beaney M, Cristofanilli M, Andre F, Loi S, Loibl S, et al. Plasma ESR1 mutations and the treatment of estrogen receptor-positive advanced breast cancer. J Clin Oncol. 2016;34(25):2961–8.
54. Spoerke JM, Gendreau S, Walter K, Qiu J, Wilson TR, Savage H, Aimi J, Derynck MK, Chen M, Chan IT, et al. Heterogeneity and clinical significance of ESR1 mutations in ER-positive metastatic breast cancer patients receiving fulvestrant. Nat Commun. 2016;7: 11579.
55. Fujiki Y, Yamamoto Y, Sueta A, Yamamoto-Ibusuki M, Goto-Yamaguchi L, Tomiguchi M, Takeshita T, Iwase H. APOBEC3B gene expression as a novel predictive factor for pathological complete response to neoadjuvant chemotherapy in breast cancer. Oncotarget. 2018;9(55):30513–26.
56. Martinez-Saez O, Chic N, Pascual T, Adamo B, Vidal M, Gonzalez-Farre B, Sanfeliu E, Schettini F, Conte B, Braso-Maristany F, et al. Frequency and spectrum of PIK3CA somatic mutations in breast cancer. Breast Cancer Res. 2020;22(1):45.
57. Nakamura K, Ishikawa M, Kawano R, Aimono E, Mizuno T, Nohara S, Tanishima S, Hayashi H, Nishihara H, Keio Ple SG. Characterizing multi-PIK3CA mutations across cancer types: toward precision oncology. Cancer Med. 2024;13(14):e70052.
58. Brito Baleeiro R, Liu P, Chard Dunmall LS, Di Gioia C, Nagano A, Cutmore L, Wang J, Chelala C, Nyambura LW, Walden P, et al. Personalized neoantigen viro-immunotherapy platform for triple-negative breast cancer. J Immunother Cancer. 2023;11(8):e007336.
59. Chen L, Han X. Anti-PD-1/PD-L1 therapy of human cancer: past, present, and future. J Clin Invest. 2015;125(9):3384–91.
60. Corti C, Giachetti PPMB, Eggermont AMM, Delaloge S, Curigliano G. Therapeutic vaccines for breast cancer: Has the time finally come? Eur J Cancer. 2022;160:150–74.
61. Braun DA, Moranzoni G, Chea V, McGregor BA, Blass E, Tu CR, Vanasse AP, Forman C, Forman J, Afeyan AB, et al. A neoantigen vaccine generates antitumour immunity in renal cell carcinoma. Nature. 2025;639(8054):474–82.

Publisher's Note